IEEE Access
Multidisciplinary : Rapid Review : Open Access Journal

Received October 23, 2018, accepted November 14, 2018, date of current version March 12, 2019.

Digital Object Identifier 10.1109/ACCESS.2018.2889724

A Generalized Capacitance Model of RF MEMS Switch by Considering the Fringing Effect

K. SRINIVASA RAO[1], (Member, IEEE), B. V. S. SAILAJA[1], K. GIRIJA SRAVANI[1,2], K. V. VINEETHA[1], P. ASHOK KUMAR[1], D. PRATHYUSHA[1], G. SAI LAKSHMI[1], C. H. GOPI CHAND[1], AND KOUSHIK GUHA[2], (Member, IEEE)

[1]MEMS Research Center, Department of Electronics and Communication Engineering, Koneru Lakshmaiah Education Foundation (Deemed to be University), Guntur 522502, India

[2]National MEMS Design Center, Department of Electronics and Communication Engineering, National Institute of Technology, Silchar 788010, India

Corresponding author: K. Srinivasa Rao (srinivasakarumuri@gmail.com)

The authors would like to thank to NMDC supported by NPMASS, for providing the necessary computational tools.

ABSTRACT Movable suspended microstructures are common features of sensors and devices in the field of micro electro mechanical systems (MEMS). This paper addresses the study of approach to model the capacitance for the crab-type meander-based RF MEMS shunt switch with etching holes on the beam. The presented paper evaluates the parallel-plate capacitance and fringing-field capacitance caused by the etching holes on the beam and introduces empirical formulae. From the literature study, an accurate empirical formula is presented. The capacitance involves a parallel plate and a fringing field. The parallel-plate capacitance term is proposed by the authors of this work; the fringing-field capacitance term is adopted from previous work. The proposed accurate empirical capacitance formulae are derived by curve fitting the simulated values through the commercially available FEM solver. The two existing benchmark models of fringing-field capacitance are used to modify the perforated MEMS switch to obtain the proposed formula. With the existing models and presented formula, the capacitances are computed for a wide range of dimensions; the simulated results of the presented formula are validated with the calculated results. The deviation of the presented formula has an error estimation of $\pm 0.1\%$. The variation of the capacitance with different deictic thicknesses and errors is estimated and analyzed for the presented formula. The Mejis model is found to be satisfactory for a lower air gap and a 1-μm-thick beam. The Yang's model is sufficient for a higher air gap and a large number of etching holes. The proposed formulae are good for the ligament efficiency $\mu \leq 0.5$, with thickness >1 μm, and the deviation of error estimation is within $\pm 5\%$.

INDEX TERMS Fixed-fixed beam, etching holes, ligament efficiency, RF MEMS, parallel-plate capacitance, fringing-field capacitance.

I. INTRODUCTION

The RF MEMS switch replaces traditional devices such as PIN and FET switches because of additional features such as high linearity and less power consumption [1]–[3]. The beam is modified using the meander structured and perforations [21], [23]. A switch with perforations improves the overall switching time of the device, but the capacitance becomes affected. To suspend the deforming beam, it is necessary to etch the sacrificial layer. Specifically, few microstructures appear large, and the microstructures must have many holes to uniformly enhance the etchant [4], [5]. The literature shows that etching holes have greater effect on the electrical and mechanical characteristics of the switch [6], [7]. For some micro structures, etchant holes decrease the parallel-plate capacitance but increase the fringing-field capacitance because of the inner perimeters of the holes [8]–[12]. The perforations make the capacitance evaluation more difficult. Some studies in the literature are related to the fringing capacitances of two- and three-dimensional devices without etching holes. In RF devices, one of the modeling aspects is the capacitance. Few works are related to the evaluation of capacitance modeling with etching holes [13]–[16].Therefore; the authors of this work present an empirical formula with the consideration of etching holes to evaluate the fringing-field capacitance. [17], [18].The micro structural range is too narrow for practical application in sensors and MEMS devices [19], [20]. In the literature, few works are related to the parallel-plate capacitance, and no literature evaluates the parallel-plate capacitance using the ligament efficiency. Therefore, by modifying the previous literature, this work presents the accurate empirical formula to compensate the parallel-plate capacitance for etching holes with different ranges of validity. Modeling is an important aspect for the advancement of the switch. Thus, the capacitance modeling has a prominent role because holes are etched on the beam to release the sacrificial layer during fabrication. Distinctive types of capacitance models have been discussed for various parameters, but few studies discussed the following areas. (1) The combination of Palmer's equation and a hybrid formula represents the edge fringing effect for the capacitance computation [21]. (2) Yang's formula [22] represents the fringing effect by accounting for the beam thickness, but it does not consider the etching holes on the beam; thus, the fringing because of the perforations is not considered. (3) Mejis Fokkema showed a changed approach considering etching holes for the switch, but the oxide layer on the bottom plate is not considered [23]. (4) Iannacci et al. built a semi-empirical equation to represent the fringing effect on the edges of the beam and edges of the etched holes because of the finite-plate dimensions in 6-DOF and 4-DOF rigid models; however, in the 4DOF model, the finite dimensions of the top plate were ignored [24]–[26]. Among these models, Yang and Mejis' models indicate good consistency for the beam-type structure with etched holes, but they do not consider the ligament efficiency. The fringing capacitance relies on various components such as the beam thickness, air gap, dielectric thickness, hole dimensions and number of holes, which incorporates the ligament efficiency. Therefore, the authors of this work frame a new analytical model for the capacitance.

This report presents an improved capacitance model of the one-degree-of-freedom parallel-plate capacitance considering the ligament efficiency. The capacitance plays vital role in RF MEMS switches. Because of the capacitance, the switch charging and discharging vary, and the switching speed of the switch may be affected. Therefore, capacitance modeling is an important factor for RF MEMS switches. According to the literature, two models are adopted for the presented model. Yang and Mejis' models have limitations in certain conditions because they do not consider the ligament efficiency, which depends on the hole dimension. The capacitance includes parallel-plate and fringing field capacitances. The authors of this work propose an accurate model for the parallel-plate capacitance using the ligament efficiency. The fringing-field term is adopted from the existing Mejis model because it shows better results than Yang's model. The error is less than 0.1% for the presented model.

II. METHOD

A. MODEL DESCRIPTION

The structural schematic of the RF MEMS shunt switch in the CPW design is shown in Fig. 1. The switch consists of a movable beam; the signal line of the CPW design has a thin dielectric td with relative permittivity to avoid the contact of the beam with the signal line when the switch is in actuation mode. [16], [22], [24].

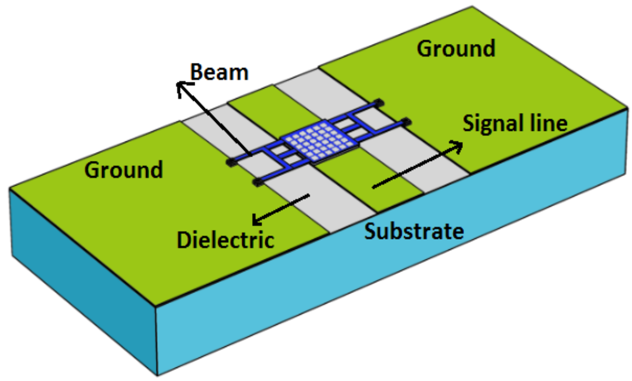

FIGURE 1. RF MEMS shunt switch with etching holes on the beam and crab-type meanders.

Furthermore, this switch is a critical factor in enhancing the capacitance of the structure. [35], [36]. When a force is applied to the beam because the voltage switch exceeds the spring restoring force, the beam begins to deform towards the signal line. The following section discusses the switch and a top view of the switch with the configuration. Four crab-type meanders are presented for all sides of the switch over the signal line.

TABLE 1. Specifications of the switch.

Parameter	Symbol	Dimensions(μm)
Width of the beam	w	80 μm
Width of signal line	W	80 μm
Dielectric thickness	t_d	(0.1-0.5) μm
Beam thickness	t_b	1 μm
Air gap	d	3.3 μm
Length of the beam	L	80 μm
Dimension of the hole	W_h	(3-8) μm
Hole count	$(n_l * n_w)$	Depends on μ
Dielectric constant	ε_r	14
Young's modulus	E	79 GPa

The parameters in Table 1 are discussed in detail.

W = Width of the beam
w = Length of the beam or width of the signal line
L = Total length of the beam including the meander section
d = Distance between the top and bottom electrodes
W_h = Dimension of the etched hole on the beam along the length and width

n_l = Number of etched holes along the beam length
n_w = Number of holes along the beam width
t_d = Thickness of the dielectric
t_b = Thickness of the plate

The existing formula for the analytical model of the capacitance for the shunt switch with parallel-plate thickness t [12], [14], [15] was proposed by Yang and is discussed in the following section.

$$C = \frac{\in w}{d}\left[1 + \frac{2d}{\pi w}\ln\left(\frac{\pi w}{d}\right) + \frac{2d}{\pi w} \times \ln\left(1 + \frac{2t}{d} + 2\sqrt{\left(\frac{t}{d} + \frac{t^2}{d^2}\right)}\right)\right] \quad (1)$$

C = Capacitance per unit length
d = Air gap between the electrodes
t = Thickness of the plate
γ_r = Dielectric constant of the dielectric medium

$\frac{\in w}{d}$: Parallel-plate capacitance
$\frac{\in w}{d} \times \frac{2d}{\pi w}\ln\left(\frac{\pi w}{d}\right)$: Fringing because of the finite dimension of the beam
$\frac{\in w}{d} \times \frac{2d}{\pi w}\ln\left(1 + \frac{2t}{d} + 2\sqrt{\left(\frac{t}{d} + \frac{t^2}{d^2}\right)}\right)$: Fringing because of the thickness of the beam.

The parallel-plate capacitor is formed by the overlapping of the signal line and the beam in capacitive shunt switches. The perforated holes on the beam can be modeled as individual capacitor. The total capacitance of the switch can be estimated by subtracting the perforated hole capacitance from the total beam capacitance of the switch considering the fringing effect. Thus, the empirical formula has three terms: (a) parallel-plate capacitance due to the edge of the beam and the thickness between the plate and the signal line; (b) capacitance due to the holes on the beam; and (c) fringing capacitance due to the holes. To model the total capacitance of the beam, the modified Yang formula is

$$C = a - b + c$$

where

$$a = \frac{\in wW}{\left(d + \frac{t_d}{\varepsilon_r}\right)} + \frac{2 \in w}{\pi}\left[\ln\left(\frac{\pi w}{\left(d + \frac{t_d}{\varepsilon_r}\right)}\right) + \ln\left(1 + \frac{2t_b}{\left(d + \frac{t_d}{\varepsilon_r}\right)}\right] + 2\sqrt{\left(\frac{t_b}{\left(d + \frac{t_d}{\varepsilon_r}\right)} + \frac{t_b^2}{\left(d + \frac{t_d}{\varepsilon_r}\right)^2}\right)}\right)\right].$$

$$b = n_l \times n_w \times \frac{\in w_h^2}{\left(d + \frac{t_d}{\varepsilon_r}\right)}$$

$$c = \frac{2 \times n_l \times n_w \times \in_0 \times w_h}{\pi} \times \left[\ln\left(\frac{\pi w_h}{\left(d + \frac{t_d}{\varepsilon_r}\right)}\right) + \ln\left(1 + \frac{2t_b}{\left(d + \frac{t_d}{\varepsilon_r}\right)} + 2\sqrt{\frac{2t_b}{\left(d + \frac{t_d}{\varepsilon_r}\right)} + \frac{t_b^2}{\left(d + \frac{t_d}{\varepsilon_r}\right)^2}}\right)\right] \quad (2)$$

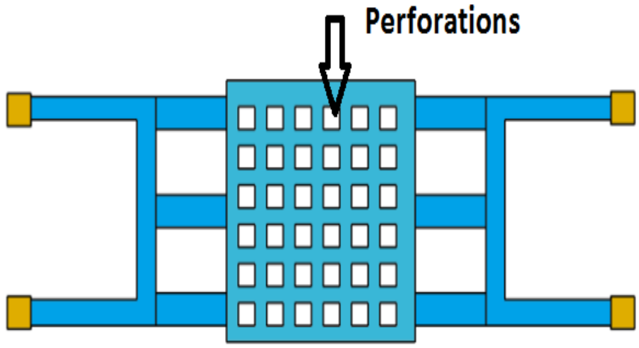

FIGURE 2. Top view of the switch with perforations on the beam.

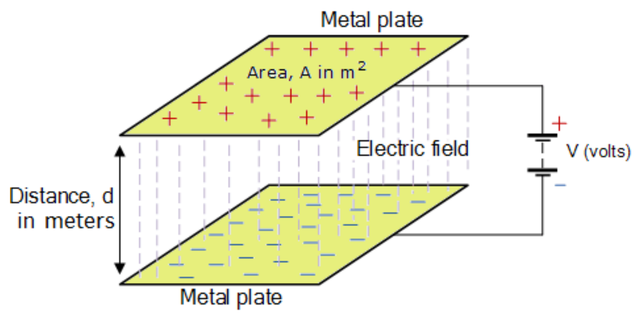

FIGURE 3. Electric field lines because of the parallel-plate capacitance.

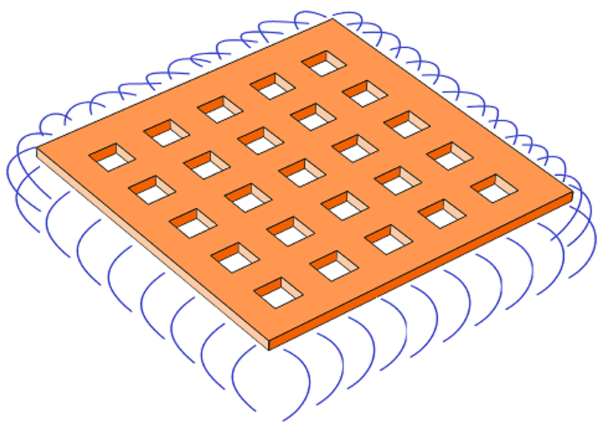
FIGURE 4. Effect of the fringing field on the top view of the beam with etched holes.

Total capacitance C = Capacitance of the fringing field with non-perforated plate-capacitance because of the holes without a fringing field + Fringing field capacitance because

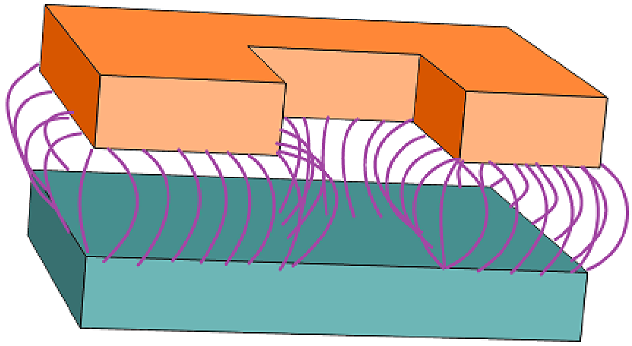

FIGURE 5. Inner view of the etched hole with the effect of the fringing field.

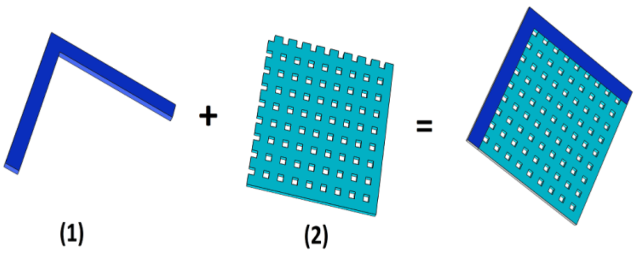

FIGURE 6. Parallel-plate capacitance calculation by adding parts 1 and 2.

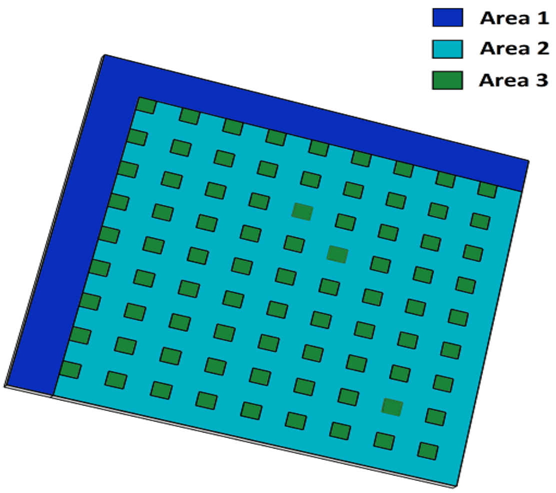

FIGURE 7. Different areas in the calculation of the parallel-plate capacitance.

of the holes.

$$C_{Total} = \varepsilon_0 W \left[\frac{w}{\left(d + \frac{t_d}{\varepsilon_r}\right)} + 0.77 + 1.06 \left(\frac{w}{\left(d + \frac{t_d}{\varepsilon_r}\right)} \right)^{\frac{1}{2}} + 1.06 \left(\frac{t_b}{\left(d + \frac{t_d}{\varepsilon_r}\right)} \right)^{\frac{1}{2}} + \right] - \frac{n_l n_w \in_0 w_h^2}{\left(d + \frac{t_d}{\varepsilon_r}\right)}$$

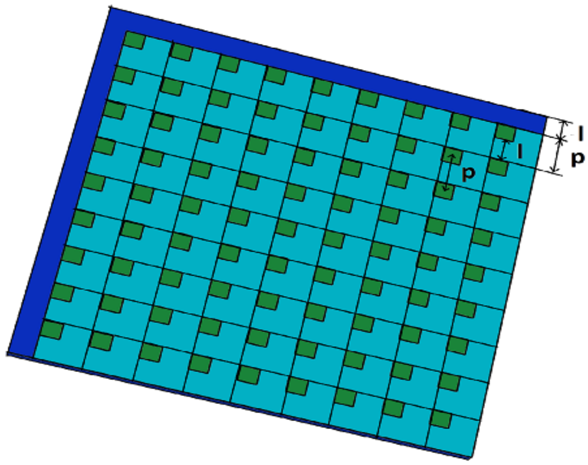

FIGURE 8. Different areas in the calculation of the parallel-plate capacitance.

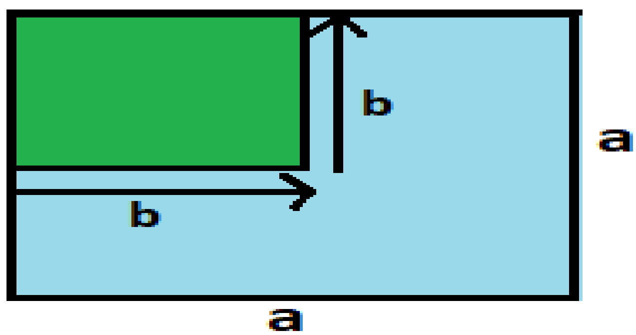

FIGURE 9. Defining percentage of area using the ligament efficiency.

$$+ n_l n_w \in_0 w_h \left[0.77 + 1.06 \left(\frac{w}{\left(d + \frac{t_d}{\varepsilon_r}\right)} \right)^{\frac{1}{2}} + 1.06 \left(\frac{t_b}{\left(d + \frac{t_d}{\varepsilon_r}\right)} \right)^{\frac{1}{2}} \right] \quad (3)$$

B. CAPACITANCE COMPENSATION TERMS FOR ETCHING HOLES

The cross-section view of the shunt capacitive switch is shown in this section. The electric field is composed of two parts: a uniform field under the bottom surface of the plate and fringing field because of the top surface and sidewalls of the structure. Therefore, the total capacitance is the sum of the parallel-plate capacitance of the bottom surface of the structure and the fringing capacitance of the sidewalls and top surface of the structure. Etchants are uniformly distributed on the beam to remove the sacrificial layer in the fabrication process. The entire structure can be divided into no square modules, and we analyze the fringing capacitance of each square module. The capacitance can be expressed as $C = C_p + C_f$.

TABLE 2. Estimation of the error analysis with the ligament efficiency.

Variables		Cup (fF) (Simulated)	Cup (fF) (Yang model)		Cup (fF) (Mejis model)		Cup (fF) (Proposed model)	
μ	t_d(μm)	(fF)	(fF)	% of error	(fF)	% of error	(fF)	% of error
0.625	0.1	28.1	18.9	32.6	25.8	10.0	18.8	15.5
	0.2	27.1	19.1	29.5	25.7	6.87	18.8	15.3
	0.3	27.0	19.3	28.7	25.7	6.66	18.8	15.5
	0.4	26.9	19.4	27.9	25.6	6.45	18.8	15.2
	0.5	27.6	19.5	29.4	25.6	8.96	18.7	14.5
0.55	0.1	28.6	18.7	34.7	24.9	12.9	20.5	18.6
	0.2	27.8	18.9	32.1	24.9	10.5	20.4	16.3
	0.3	27.7	19.0	31.3	24.8	10.3	20.4	16.2
	0.4	27.5	19.2	30.6	24.8	10.2	20.4	16.6
	0.5	27.5	19.3	29.9	24.7	10.0	20.4	15.8
0.5	0.1	27.9	18.3	34.3	24.0	13.9	21.0	16.7
	0.2	27.8	18.3	33.4	24.0	13.7	21.0	16.5
	0.3	27.7	18.3	32.6	23.9	13.5	21.0	16.3
	0.4	27.5	18.8	31.7	23.9	13.9	21.0	16.7
	0.5	28.0	18.9	32.5	23.9	14.7	20.9	17.4
0.45	0.1	27.5	17.8	35.3	22.8	16.8	22.4	23.1
	0.2	28.0	18.0	35.6	22.8	16.6	22.4	23.1
	0.3	27.6	18.2	34.5	22.7	16.4	22.3	23.0
	0.4	27.2	18.4	33.8	22.7	16.2	22.3	22.8
	0.5	27.1	18.5	31.3	22.7	16.0	22.3	22.6
0.41	0.1	27.4	17.4	36.3	22.8	16.8	22.4	23.3
	0.2	27.3	17.6	35.4	22.8	16.6	22.4	23.1
	0.3	27.2	17.8	34.5	22.7	16.4	22.3	23.0
	0.4	27.1	17.9	33.2	22.7	16.2	22.3	22.8
	0.5	27.1	17.9	33.2	22.7	16.2	22.3	22.8
0.38	0.1	26.9	16.7	37.8	22.5	16.4	23.9	19.8
	0.2	26.9	17.0	36.9	22.4	16.5	23.9	19.9
	0.3	26.8	17.1	36.0	22.4	16.3	23.8	19.8
	0.4	26.7	17.3	35.2	22.4	16.1	23.8	19.9
	0.5	26.5	17.4	34.2	22.4	15.6	23.8	19.1

TABLE 3. Comparison of different models for different air gaps and dielectric thicknesses in the up state with $\mu = 0.41$ and $t_b = 2$ μm.

Variables		%error of (Proposed)	%error of (Yang)	%error of (Mejis)
d(μm)	t_d(μm)	Model%	Model%	Model%
3	0.1	0.21	18.8	10.2
3	0.2	0.06	17.4	10.6
3	0.3	0.51	17.0	9.94
3	0.4	0.21	15.6	10.8
3	0.5	0.06	15.0	10.6

C. PARALLEL-PLATE CAPACITANCE

In the parallel-plate capacitor, charges are carried by the charge-carrying plate. The parallel-plate capacitance depends on the area. The total area of the beam depends on the ligament efficiency. The area of the beam is directly proportional to the capacitance but inversely proportional to the ligament efficiency. If the observed increase in ligament efficiency area can be reduced, the capacitance also reduces. The parallel-plate capacitance is formed under the bottom surface

TABLE 4. Estimation of the error analysis with the ligament efficiency, beam thickness 0.8 μm, t_d (d = 3 μm) and hole size of (3-8μm).

Variables		Cup (fF) (Simulated)	Cup (fF) Yang model		Cup (fF) Mejis model		Cup (fF) Proposed model	
μ	t_d(μm)	(fF)	(fF)	% of error	(fF)	% of error	(fF)	% of error
0.625	0.1	26.9	19.1	28.9	25.6	4.88	19.1	10.9
	0.2	26.8	19.3	27.9	25.5	4.67	19.1	10.7
	0.3	26.7	19.5	27.1	25.5	4.45	19.0	10.5
	0.4	26.7	19.6	26.7	25.5	4.59	19.0	10.6
	0.5	26.6	19.7	26.0	25.4	4.38	19.0	10.4
0.55	0.1	26.9	18.9	29.8	25.2	6.26	20.7	12.5
	0.2	26.7	19.1	28.5	25.2	5.69	20.7	12
	0.3	26.6	19.2	27.7	25.1	5.47	20.7	11.8
	0.4	26.6	19.4	27.2	25.1	5.61	20.6	11.9
	0.5	26.5	19.5	26.5	25.1	5.39	20.6	11.7
0.5	0.1	26.7	18.5	30.6	24.3	8.90	21.3	11.9
	0.2	26.6	18.7	29.6	24.3	8.69	21.2	11.7
	0.3	26.5	18.9	28.8	24.3	8.48	21.2	11.5
	0.4	26.4	19.0	28.1	24.2	8.26	21.2	11.3
	0.5	26.3	19.1	27.4	24.2	8.04	21.1	11.1
0.45	0.1	26.4	18.0	31.7	24.5	7.34	23.5	11.9
	0.2	26.3	18.3	30.6	24.4	7.12	23.5	11.7
	0.3	26.2	18.4	29.6	24.4	6.89	23.4	11.5
	0.4	26.2	18.6	29.0	24.4	7.01	23.4	11.6
	0.5	26.1	18.7	28.2	24.3	6.78	23.4	11.4
0.41	0.1	26.3	17.7	32.9	23.1	12.1	22.6	14.0
	0.2	26.2	17.9	31.8	23.1	11.9	22.6	13.8
	0.3	26.1	18.0	31.0	23.0	11.7	22.6	13.6
	0.4	26.1	18.1	30.5	23.0	11.8	22.5	13.7
	0.5	26	18.3	29.8	23.0	11.6	22.5	13.5
0.38	0.1	25.9	17.0	34.5	22.8	11.9	24.2	15.7
	0.2	25.8	17.2	33.3	22.8	11.7	24.1	15.5
	0.3	25.7	17.4	32.4	22.8	11.4	24.1	15.2
	0.4	25.7	17.5	31.8	22.7	11.5	24.1	15.4
	0.5	25.6	17.7	31.0	22.7	11.3	24.0	15.1

TABLE 5. Comparison of the up-state capacitance with various air gaps and dielectric thicknesses of the proposed model; $\mu = 0.3$; $t_b = 2$ μm.

Variables		Cup (fF)		Error
d(μm)	t_d(μm)	(Simulated)	(Calculated)	deviation%
3	0.1	22.7	25.0	0.37
3	0.2	22.6	24.9	0.07
3	0.3	22.6	24.9	0.2
3	0.4	22.5	24.8	0.09
3	0.5	22.4	24.8	0.41

of the structure. C_p is calculated by the ideal parallel-plate capacitance formula.

D. FRINGING FIELD CAPACITANCE

It is necessary to maintain the smallest capacitance to pass the high frequency for the switch. The fringing field capacitance purely depends on the etched holes on the beam, which are related to their sizes. In the perforated shunt capacitive shunt switch, the electric field passes through the etched holes and alters the total capacitance of the beam. The fringing capacitance appears because of the sidewalls and top surface

TABLE 6. Error deviation with the ligament efficiency, beam thickness 1 μm, t_d = 0.1-0.5 μm, d = 3 μm and wh = 3-8μm.

VARIABLES		CUP (FF) (SIMULATED)	CUP (FF) YANG MODEL		CUP (FF) MEJIS MODEL		CUP (FF) PROPOSED MODEL	
μ	T_D(μM)	(FF)	(FF)	% OF ERROR	(FF)	%OF ERROR	(FF)	% OF ERROR
	0.1	26.1	19.2	26.2	25.8	1.29	19.2	7.64
	0.2	26.1	19.4	25.5	25.7	1.43	19.2	7.78
0.625	0.3	26.0	19.6	24.6	25.7	1.20	19.2	7.57
	0.4	25.9	19.7	23.9	25.6	0.96	19.1	7.35
	0.5	25.9	19.8	23.5	25.6	1.11	19.1	7.49
	0.1	26.2	19.0	27.4	25.4	3.05	20.9	9.63
	0.2	26.1	19.2	26.3	25.4	2.82	20.8	9.42
0.55	0.3	25.9	19.4	25.2	25.3	2.21	20.8	8.86
	0.4	25.9	19.5	24.7	25.3	2.35	20.8	8.99
	0.5	25.8	19.6	24.0	25.3	2.11	20.7	8.78
	0.1	26.1	18.6	28.5	24.5	6.12	21.4	9.30
	0.2	25.9	18.8	27.2	24.5	5.53	21.4	8.73
0.5	0.3	25.9	19.0	26.6	24.4	5.67	21.3	8.86
	0.4	25.8	19.1	25.9	24.4	5.44	21.3	8.64
	0.5	25.7	19.2	25.2	24.4	5.21	21.3	8.41
	0.1	25.8	18.2	29.5	24.7	4.39	23.7	9.24
	0.2	25.7	18.4	28.3	24.6	4.15	23.6	9.01
0.45	0.3	25.6	18.6	27.3	24.6	3.91	23.6	8.78
	0.4	25.5	18.7	26.5	24.6	3.66	23.5	8.55
	0.5	25.4	18.9	25.6	24.5	3.40	23.5	8.32
	0.1	25.7	16.9	34.0	23.3	9.38	22.8	1.14
	0.2	25.6	17.0	33.6	23.3	9.15	22.7	1.12
0.41	0.3	25.5	17.0	33.3	23.2	8.92	22.7	1.09
	0.4	25.5	17.0	33.2	23.2	9.05	22.7	1.11
	0.5	25.4	17.0	32.9	23.2	8.81	22.6	1.08
	0.1	25.3	17.0	32.9	23.0	9.0	24.3	1.31
	0.2	25.2	17.2	31.7	23.0	8.75	24.3	1.28
0.38	0.3	25.1	17.4	30.7	23.0	8.50	24.3	1.26
	0.4	24.9	17.5	29.5	22.9	7.89	24.2	1.20
	0.5	25.0	17.7	29.3	22.9	8.38	24.2	1.25

TABLE 7. Error estimation of the up-state capacitance in terms of ligament efficiency of the proposed model.

μ	Simulated (C_{up})	Analytical (C_{up})	%Error%
	t_d=0.3 μm, d=3 μm		
0.62	24.1	19.7	1.76
0.55	23.8	21.4	1.48
0.5	23.3	21.9	1.36
0.45	23.1	24.2	0.51
0.41	22.8	23.2	2.36
0.38	22.6	24.9	0.2

of the structure. The increase in the number of edges, which increases the fringing field, depends on the number of holes.

The effect of the number of holes and their sizes varies with the ligament efficiency. If the number of holes on the beam increases, the hole size decreases; then, there is an increase in ligament efficiency, which increases the fringing-field capacitance. The following figures depict the effects of the fringing-field effects around the sidewalls and a close view of the etched hole and the fringing field from the inner perimeters of the etching hole.

TABLE 8. c μ variation, beam thickness 2 μm, t_d = 0.1 − 0.5 μm, d = 3 μm and wh = 3-8.

Variables		Cup (fF) (Simulated)	Cup (fF) Yang model		Cup (fF) Mejis model		Cup (fF) Proposed model	
μ	t_d(μm)	(fF)	(fF)	% of error	(fF)	% of error	(fF)	% of error
	0.1	24.2	19.7	18.4	26.5	9.31	19.7	1.76
	0.2	24.1	19.9	17.3	26.4	9.60	19.7	2.03
0.625	0.3	24.1	20.1	16.7	26.4	9.44	19.7	1.87
	0.4	24.0	20.2	15.9	26.3	9.74	19.6	2.14
	0.5	23.9	20.3	15.1	26.3	10.0	19.6	2.41
	0.1	24.0	19.5	18.6	26.1	8.83	21.4	0.92
	0.2	23.9	19.7	17.4	26.1	9.12	21.4	1.21
0.55	0.3	23.8	19.9	16.5	26.0	9.42	21.4	1.48
	0.4	23.6	20.0	15.2	26.0	10.2	21.3	2.19
	0.5	23.5	20.1	14.4	26.0	10.5	21.3	2.47
	0.1	23.5	19.2	18.5	25.2	7.22	21.9	1.91
	0.2	23.5	19.3	17.7	25.2	7.06	21.9	1.63
0.5	0.3	23.3	19.5	16.4	25.1	7.83	21.9	1.36
	0.4	23.2	19.6	15.5	25.1	8.14	21.8	1.09
	0.5	23.2	19.7	15.1	25.1	7.98	21.8	1.23
	0.1	23.1	18.8	18.8	25.5	10.2	24.3	0.21
	0.2	23.0	19.0	17.4	25.4	10.6	24.2	0.06
0.45	0.3	23.1	19.2	17.0	25.4	9.94	24.2	0.51
	0.4	22.9	19.3	15.6	25.4	10.8	24.2	0.21
	0.5	22.9	19.5	15.0	25.3	10.6	24.1	0.06
	0.1	22.9	18.3	20.1	24.0	4.79	23.3	2.19
	0.2	22.9	18.5	19.3	24.0	4.65	23.3	2.05
0.41	0.3	22.8	18.6	18.2	23.9	4.96	23.2	2.36
	0.4	22.9	18.8	18.0	23.9	4.36	23.2	1.77
	0.5	22.7	18.9	16.8	23.9	5.14	23.2	2.53
	0.1	22.7	17.7	22.1	23.8	4.86	25.0	0.37
	0.2	22.6	17.9	20.7	23.8	5.22	24.9	0.07
0.38	0.3	22.6	18.1	20.0	23.7	5.08	24.9	0.20
	0.4	22.5	18.2	18.9	23.7	5.41	24.8	0.09
	0.5	22.4	18.4	18.0	23.7	5.75	24.8	0.41

E. LIGAMENT EFFICIENCY FOR THE CAPACITANCE CALCULATION

In the fabrication process, the etched holes on the beam are used to remove the sacrificial layer. The perforations on the beam increase the switching speed of the device. The smaller etched holes on the beam show a weaker effect on the capacitance. Therefore, it is important to note the effects of holes on the beam and their size variation on the total capacitance. The specification of the etched holes on the beam can be evaluated in terms of ligament efficiency μ as shown in the figure. Larger ligament efficiency corresponds to a smaller etching hole. The switch is simulated for different parameter variations of the ligament efficiency. The variation in the effect is shown in equation number-5 varying the number of etched holes and their size. The error percentage of the proposed model can be decreased with decreasing ligament efficiency by decreasing the number of holes and increasing the hole size. Thus, using the proposed model, a high accuracy can be achieved for a larger hole size. The proposed model is satisfactory for stronger fringing effects.

TABLE 9. Comparison of all capacitance models for different parameter variations.

Parameter	Yang's model	Mejis model	Proposed model
Less beam height	Not accurate	Best	Best
More beam height	Best	Not accurate	Accurate
Lower number of etching holes	Not accurate	Accurate	Accurate
Higher number of etching holes	Best	Not accurate	Best
Ligament efficiency ranges (0.3-0.5)	Accurate	Best	Best
Ligament efficiency ranges (0.5-0.8)	Best	Best	Best
Beam thickness ranges (0.5-1 µm)	Best	Best	Accurate
Beam thickness ranges (1-2.5 µm)	Accurate	Accurate	Best

F. FORMULA DERIVATION

There are four stages to infer the proposed empirical formulae for parallel-plate and fringing-field capacitances with etching holes on the beam. The first two stages involve the parallel-plate capacitance; the last two stages involve the fringing-field capacitance. First, the beam area is partitioned into two sections. From the initial segment, the area where the ligament efficiency is not affected should be considered; then, the area where the ligament efficiency is affected must be subtracted. Second, the area where the ligament efficiency is affected must be subtracted from (1-(1-μ)^2), which is the area after etching. The sum of the first two sections of the formulae is the total area to compute the parallel-plate capacitance. Third, the total fringing field of the beam without etched holes is adopted from Yang's model. Finally, the fringing field of the etching holes is adopted from Mejis' capacitance model. Combining the last two terms, we obtain the fringing capacitance (4), as shown at the bottom of this page.

Area 1- Ligament efficiency of the unaffected part.

Area 2- Ligament efficiency of the affected part, Percentage of the etched area.

Area 3- Percentage of the remaining area after etching.

The total beam fringing field should be affected because the fringing-field term is adopted from (1) Yang's formula for the fringing capacitance without etching holes and (2) Mejis formula for the fringing capacitance with etching holes. The sum of these two terms includes the total fringing-field capacitance.

The unit modules can be discussed for the parallel-plate capacitance by considering the example.

$$w_h = \mathrm{b}, \quad l = 7, \ \mathrm{P} = \mathrm{a}$$
$$\mathrm{a} = 10, \quad \mathrm{b} = 9$$
$$\text{Total area} = (\mathrm{a} * \mathrm{a}) - (\mathrm{b} * \mathrm{b}) = 91$$

The total area is calculated in terms of the ligament efficiency

$$\mu = 0.7$$
$$\text{Percentage of area etched } (1-\mu) = 0.3$$
$$\text{Percentage of area after etching } (1-(1-\mu)^2) = 1 - 0.09 = 0.91$$
$$\mu = \frac{l}{pitch}$$
$$\text{Pitch} = l + w_h$$

Therefore, by multiplying the total area with the percentage of remained area after etching, we calculate the final area.

$$\text{Final area} = 100 * 0.91 = 91$$

III. RESULTS AND DISCUSSIONS

The existing models of Yang and Mejis to compute the total capacitance of the perforated beam switch, which include

$$C = C_p + C_f$$
$$C_p = \frac{\varepsilon_0 \left[(w \times W) - ((w-l) \times (W-l)) + ((w-l) \times (W-l) \times (1-(1-\mu)^2)\right]}{\left(d + \frac{t_d}{\varepsilon_r}\right)}$$
$$C_f = \frac{2 \in W}{\pi}\left[\ln\left[\frac{\pi w}{\left[d + \frac{t_d}{\varepsilon_r}\right]}\right] + \ln\left[1 + \frac{2t_b}{\left[d + \frac{t_d}{\varepsilon_r}\right]} + 2\sqrt{\left[\frac{t_b}{\left[d + \frac{t_d}{\varepsilon_r}\right]} + \frac{t_b^2}{\left[d + \frac{t_d}{\varepsilon_r}\right]}\right]}\right]\right]$$
$$+ n_l n_w \in_0 w_h \left[0.77 + 1.06\left(\frac{w}{\left(d + \frac{t_d}{\varepsilon_r}\right)}\right)^{\frac{1}{2}} + 1.06\left(\frac{t_b}{\left(d + \frac{t_d}{\varepsilon_r}\right)}\right)^{\frac{1}{2}}\right] \quad (4)$$

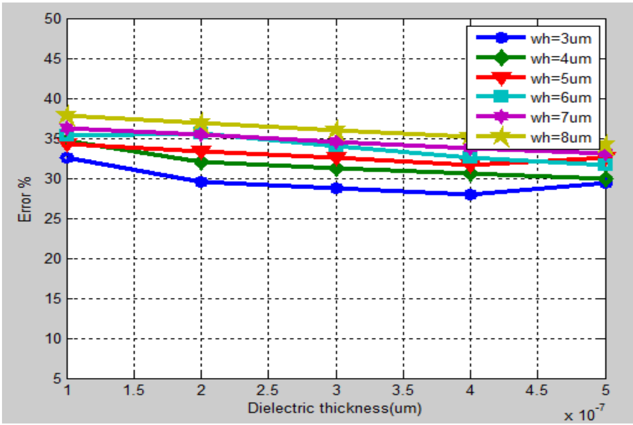

(a)

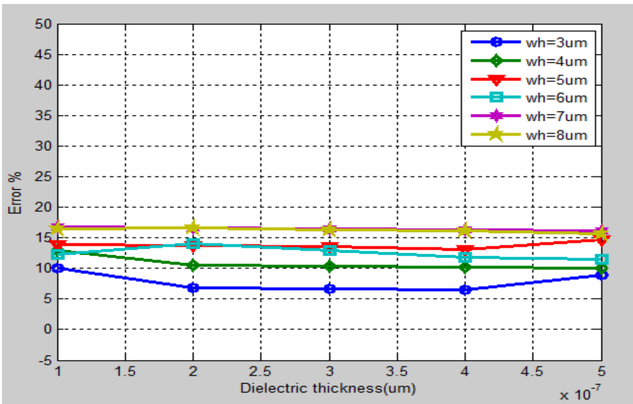

(b)

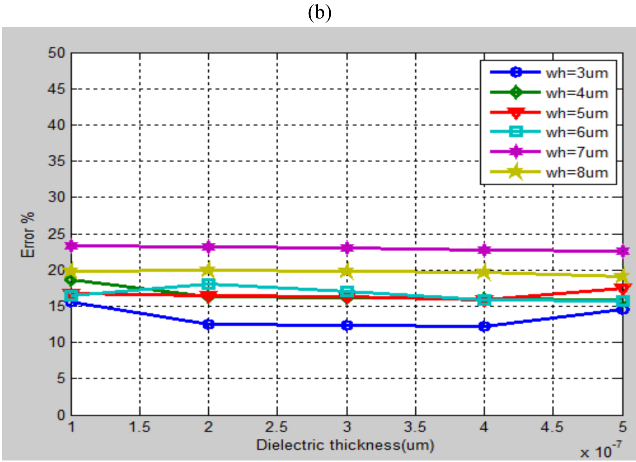

(c)

FIGURE 10. **Up-state condition of the switch with varying ligament efficiency with respect to the dielectric thickness for beam thickness 0.5 μm: (a) Yang model; (b) Mejis model; (c) Proposed model.**

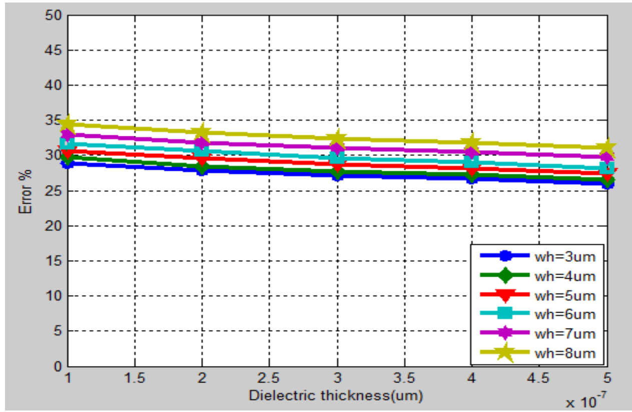

(a)

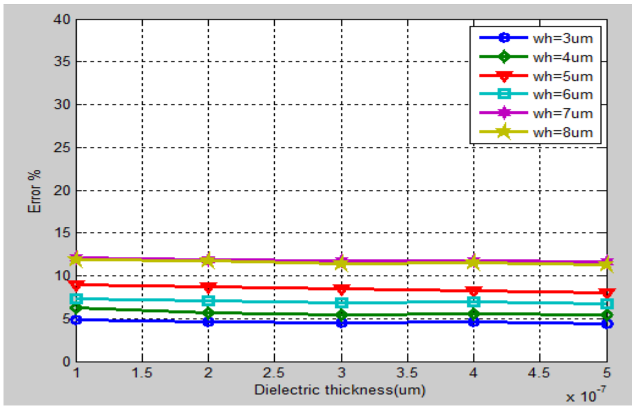

(b)

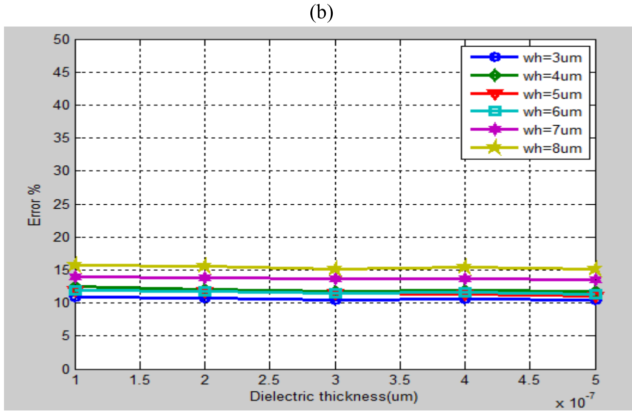

(c)

FIGURE 11. **Up-state condition of the switch in terms of the ligament efficiency with respect to the dielectric thickness for beam thickness 0.8 um: (a) Yang model; (b) Mejis model; (c) Proposed model.**

parallel-plate and fringing-field capacitances, are considered to compare with and validate the proposed model. The error analysis performance of the proposed model is validated with respect to the FEM tool as shown in Tables 2-8, and the variation in error analysis in terms of the ligament efficiency is graphically shown in Figs. 10-13.

The proposed model has good accuracy at a smaller air gap with a smaller dielectric thickness but fails at smaller beam thickness. The up-state capacitance of the perforated switch is tabulated in Tables 2-8 to discuss the variation of the beam thickness from 0.5 μm to 2 μm in terms of μ by varying the dielectric thickness. The capacitance values and their error deviation for different parameters are calculated and simulated. The theoretical calculations and simulated results show that the error deviation with respect to the previous models is not accurate for different parameters such as the beam height, beam thickness, dielectric thickness, number of holes, hole dimension, and ligament efficiency. Compared with the existing models, the error percentage is acceptable at almost every parameter variation.

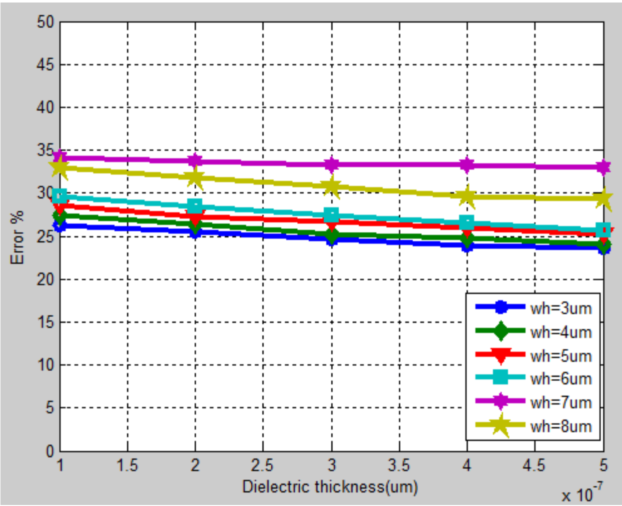

(a)

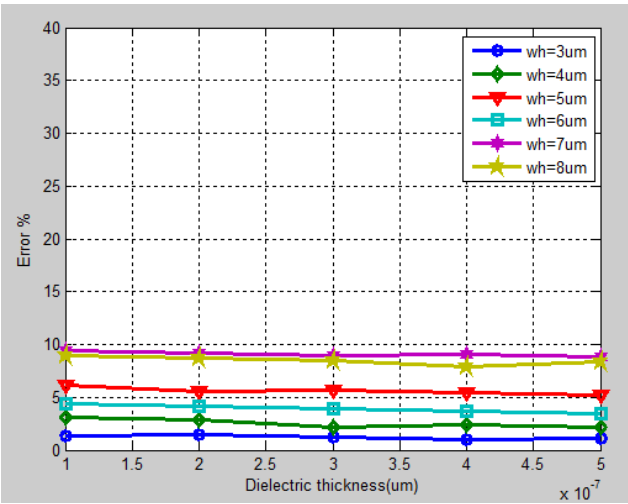

(b)

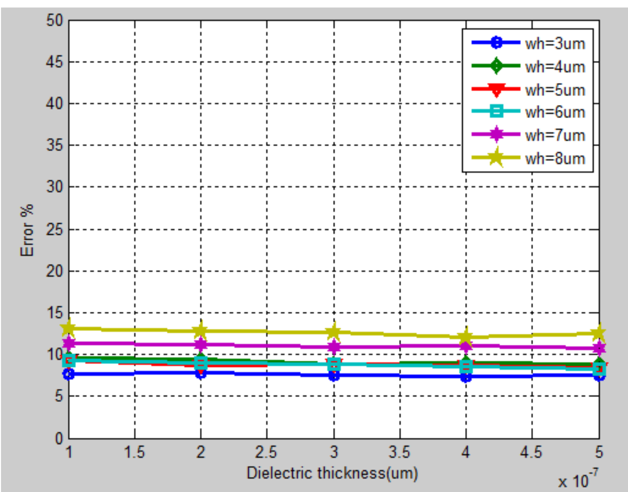

(c)

FIGURE 12. Up-state condition of the perforated switch in terms of μ with respect to dielectric thickness for beam thickness 1 μm (a) Yang model; (b) Mejis model; (c) Proposed model.

This proposed model shows good accuracy with respect to the beam thickness of 1-2 μm with an error estimation of $\pm 5\%$.

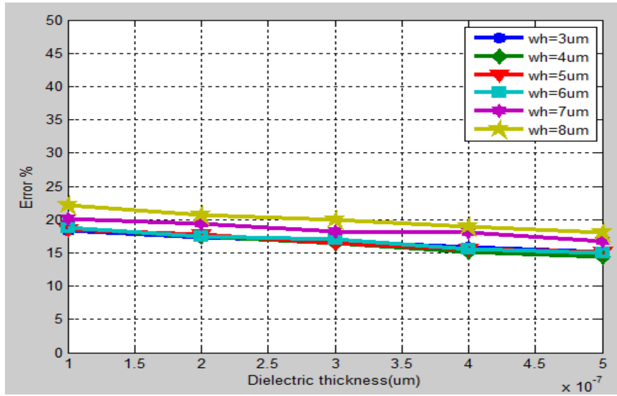

(a)

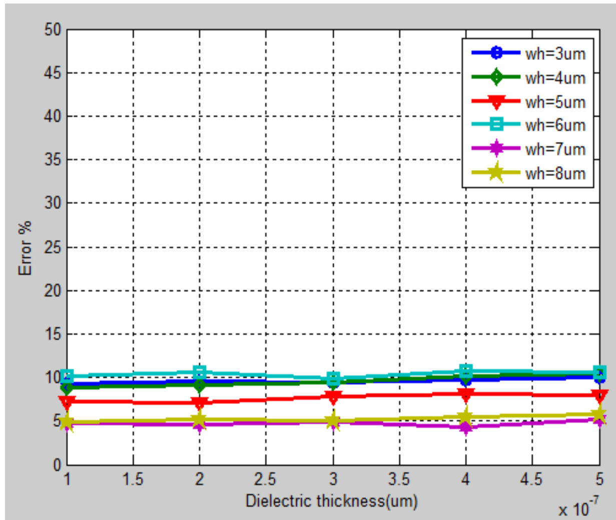

(b)

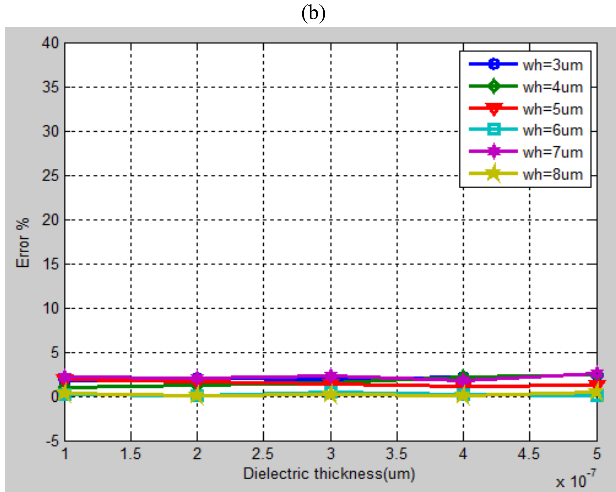

(c)

FIGURE 13. Up-state condition of the perforated switch in terms of μ with respect to the dielectric thickness for beam thickness 2 um: (a) Yang model; (b) Mejis model; (c) Proposed model.

IV. CONCLUSION

This report presents a comparative study of the error performance analysis of the proposed capacitance model, Yang capacitance model and Mejis model for the shunt capacitive switch with consideration of the fringing effect. All presented models are validated with the FEM tool and a wide range of variations, including the airgap between the electrodes, thickness of the dielectric, ligament efficiency and beam thickness in the up-state of the switch.

In this paper, a new analytical model for the parallel-plate capacitance has been proposed, and the fringing-field capacitance has been adopted from the modified Yang and Mejis models. Only 0.2% error is obtained with ligament efficiency $\mu = 0.416$. The proposed model shows good accuracy with the simulated model for the range of ligament efficiency of $0.7 > \mu > 0.45$ and beam thickness 1 μm $< t_b <$ 2.5 μm; the error is $\pm 5\%$ for the Up-state condition of the switch. he values of the proposed model and existing Mejis model are co-related at few parameters. The existing Yang model shows good accuracy with a higher air gap and more holes on the beam. Mejis model appears to be good under opposite conditions of Yang model. The proposed model shows acceptable accuracy with various parameters. Finally, we conclude that the proposed model is sufficient with lower air gap, lower di-electric thickness, higher beam thickness and more holes with less dimension. This analytical model is suitable for the analysis of the MEMS shunt capacitive switch in a given range with acceptable accuracy.

REFERENCES

[1] X. Fang, N. Myung, K. Nobe, and J. W. Judy, "Modeling the effect of etch holes on ferromagnetic MEMS," *IEEE Trans. Magn.*, vol. 37, no. 4, pp. 2637–2639, Jul. 2001.

[2] A. M. Elshurafa and E. I. El-Masry, "Effects of etching holes on capacitance and tuning range in MEMS parallel plate variable capacitors," in *Proc. 6th Int. Workshop Syst. Chip Real Time Appl.*, Cairo, Egypt, Dec. 2006, pp. 221–224.

[3] A. M. Elshurafa and E. I. El-Masry, "Design considerations in MEMS parallel plate variable capacitors," in *Proc. 50th Midwest Symp. Circuits Syst.*, Montreal, Canada, Aug. 2007, pp. 1173–1176.

[4] D.-M. Fang, X.-H. Li, Q. Yuan, and H.-X. Zhang, "Effect of etch holes on the capacitance and pull-in voltage in MEMS tunable capacitors," *Int. J. Electron.*, vol. 97, no. 12, pp. 1439–1448, 2010.

[5] W. H. Chang, "Analytical IC metal-line capacitance formulas," *IEEE Trans. Microw. Theory Techn.*, vol. MTT-24, no. 9, pp. 608–611, Sep. 1976.

[6] N. P. Van Der Meijs, and J. T. Fokkema, "VLSI circuit reconstruction from mask topology," *Integration*, vol. 2, pp. 85–119, Jun. 1984.

[7] H. Yang, "Microgyroscope and microdynamics," Ph.D. Dissertation, 2000.

[8] H. B. Palmer, "The capacitance of a parallel-plate capacitor by the Schwartz-Christoffel transformation," *Elect. Eng.*, vol. 56, no. 3, pp. 363–368, Mar. 1937.

[9] J. Iannacci, *Practical Guide to RF-MEMS*, 1st ed. Weinheim, Germany: Wiley-VCH, 2013, p. 372.

[10] J. Iannacci, L. Del Tin, R. Gaddi, A. Gnudi, and K. J. Rangra, "Compact modeling of a MEMS toggle-switch based on modified nodal analysis," in *Proc. DTIP*, Jun. 2005, pp. 411–416.

[11] J. Iannacci, L. D. Tin, R. Gaddi, A. Gnudi, and K. J. Rangra, "Compact modeling of a MEMS toggle-switch based on modified nodal analysis," in *Proc. Symp. Design, Test, Integr. Packag. MEMS/MOEMS (DTIP)*, Montreux, Switzerland, Jun. 2005, pp. 411–416.

[12] K. Shah, J. Singh, and A. Zayegh, "Modelling and analysis of fringing and metal thickness effects in MEMS parallel plate capacitors," *Proc. SPIE*, vol. 6035, p. 603511, Jan. 2006.

[13] K. Guha, M. Kumar, S. Agarwal, and S. Baishya, "A modified capacitance model of RF MEMS shunt switch incorporating fringing field effects of perforated beam," *Solid-State Electron.*, vol. 114, pp. 35–42, Dec. 2015, doi: 10.1016/j.sse.2015.07.008.

[14] V. Leus and D. Elata, "Fringing field effect in electrostatic actuators," Technion-Isr. Inst. Technol., Haifa, Israel, Tech. Rep. ETR-2004-2, May 2004.

[15] W. Jerry and P. A. Saraswathi, "A novel design of serpentine structure for enhanced performance of MEMS based pressure sensors," *Int. J. Instrum., Control Automat.*, vol. 2, no. 1, pp. 23–26, 2013.

[16] A. Bendali, R. Labedan, F. Domingue, and V. Nerguizian, "Holes effects on RF MEMS parallel membranes capacitors," in *Proc. IEEE CCECE/CCGEI*, Ottawa, Canada, May 2006, pp. 2140–2143.

[17] G. M. Rebeiz, *RF MEMS: Theory, Design, and Technology*, 3rd ed. New Jersey, NJ, USA: Wiley, 2003.

[18] V. L. Rabinovich, R. K. Gupta, and S. D. Senturia, "The effect of release-etch holes on the electromechanical behaviour of MEMS structures," in *Proc. Int. Solid State Sensors Actuat. Conf.*, Chicago, IL, USA, Jun. 1997, pp. 1125–1128.

[19] T. Sakurai and K. Tamaru, "Simple formulas for two- and three-dimensional capacitances," *IEEE Trans. Electron Devices*, vol. ED-30, no. 2, pp. 183–185, Feb. 1983.

[20] R. C. Batra, M. Porfiri, and D. Spinello, "Electromechanical model of electrically actuated narrow microbeams," *J. Microelectromech. Syst.*, vol. 15, no. 5, pp. 1175–1189, Oct. 2006.

[21] W.-C. Chuang, C.-W. Wang, W.-C. Chu, P.-Z. Chang, and Y.-C. Hu, "The fringe capacitance formula of microstructures," *J. Micromech. Microeng.*, vol. 22, no. 2, 2012, Art. no. 025015.

[22] W.-H. Tu, W.-C. Chu, C.-K. Lee, P.-Z. Chang, and Y.-C. Hu, "Effects of etching holes on complementary metal oxide semiconductor–microelectromechanical systems capacitive structure," *J. Intell. Mater. Syst. Struct.*, vol. 24, no. 3, pp. 310–317, 2012.

[23] A. L. Roy, A. Bhattacharya, R. R. Chaudhuri, and T. K. Bhattacharyya, "Analysis of the pull-in phenomenon in microelectromechanical varactors," in *Proc. 25th Int. Conf. VLSI Design*, 2012, pp. 185–190.

[24] M. Bedier and R. AbdelRassoul, "Analysis and simulation of serpentine suspensions for MEMS applications," *Int. J. Mater. Sci. Eng.*, vol. 1, no. 2, pp. 82–85, Dec. 2013.

[25] K. G. Sravani and K. S. Rao, "Analysis of RF MEMS shunt capacitive switch with uniform and non-uniform meanders," *Microsyst. Technol.*, vol. 24, no. 2, pp. 1309–1315, Feb. 2018.

[26] K. B. Lee, "The theoretical static response of electrostatic fixed–fixed beam microactuators," *Smart Mater. Struct.*, vol. 17, no. 6, 2008, Art. no. 065017.

[27] D. Mardivirin, D. Bouyge, A. Crunteanu, A. Pothier, and P. Blondy, "Study of residual charing in dielectric less capacitive MEMS switches," in *IEEE MTT-S Int. Microw. Symp. Dig.*, Jun. 2008, pp. 33–36.

[28] P. Blondy *et al.*, "Dielectric less capacitive MEMS switches," in *IEEE MTT-S Int. Microw. Symp. Dig.*, vol. 2, Jun. 2004, pp. 573–576.

[29] S.-C. Shen and M. Feng, "Low actuation voltage RF MEMS switches with signal frequencies from 0.25 GHz to 40 GHz," in *Int. Electron Devices Meeting Tech. Dig.*, Dec. 1999, pp. 689–692.

[30] J. B. Muldavin and G. M. Rebeiz, "High-isolation CPW MEMS shunt switches. 1. Modeling," *IEEE Trans. Microw. Theory Techn.*, vol. 48, no. 6, pp. 1045–1052, Jun. 2000.

[31] C. Goldsmith, T.-H. Lin, B. Powers, W.-R. Wu, and B. Norvell, "Micromechanical membrane switches for microwave applications," in *IEEE MTT-S Int. Microw. Symp. Dig.*, vol. 1, May 1995, pp. 91–94.

[32] L. L. Mercado, S.-M. Kuo, T.-Y. T. Lee, and L. Liu, "Mechanics-based solutions to RF MEMS switch stiction problem," *IEEE Trans. Compon. Packag. Technol.*, vol. 27, no. 3, pp. 560–567, Sep. 2004.

[33] B. Zhang and D. Fang, "Modeling and modification of the parallel plate variable MEMS capacitors considering deformation issue," *Mechanism Mach. Theory*, vol. 44, pp. 647–655, Apr. 2009.

[34] C. Ak and A. Yildiz, "An inversely designed model for calculating pull-in limit and position of electrostatic fixed-fixed beam actuators," *Math. Problems Eng.*, vol. 2014, Aug. 2014, Art. no. 391942.

[35] K. B. Lee, *Principles of Microelectromechanical Systems*, Hoboken, NJ, USA: Wiley, 2011.

[36] D. Mardivirin, A. Pothier, A. Crunteanu, B. Vialle, and P. Blondy, "Charging in dielectricless capacitive RF-MEMS switches," *IEEE Trans. Microw. Theory Techn.*, vol. 57, no. 1, pp. 231–236, Jan. 2009.

K. SRINIVASA RAO (M'17) was born in Andhra Pradesh, India. He received the master's and Ph.D. degrees from Central University. He is currently working as a Professor, and also the Head of the Microelectronics Research Group, Department of Electronics and Communication Engineering, Koneru Lakshmaih Education Foundation (Deemed to be University), Guntur, India. His current research areas are MEMS-based reconfigurable antenna's actuators, bio-MEMS, RF MEMS switches, and RF MEMS filters. He is a member of the IETE and ISTE. He received the Young Scientist Award from the Department of Science and Technology, Government of India, in 2011. He also received the UGC Major Research Project, in 2012. He received the Early Career Research Award from SERB, Government of India, in 2016. He is currently working on the MEMS project worth of 40 Lakhs, funded by SERB, Government of India. He has published over 94 international research publications and presented over 45 conference technical papers around the world. He has collaborated his research work with NIT's, Central Universities, IIT's, and so on. Under his guidelines, three Ph.D. Scholars has been awarded, and seven Ph.D. Scholars are currently working with him.

B. V. S. SAILAJA was born in Andhra Pradesh, India. She received the bachelor's degree in electronics and communication engineering from Anna University, in 2012, and the master's degree in VLSI from KL University, in 2018, where she is currently pursuing the Ph.D. degree on MEMS research domain. She has published 11 International research publications and presented over three conference technical papers around the world.

K. GIRIJA SRAVANI was born in Andhra Pradesh, India. She received the bachelor's degree in electronics and communication engineering, and the master's degree in VLSI and embedded systems from JNTUK. She is currently pursuing the Ph.D. degree on MEMS research domain with the National Institute of Technology, Silchar. She is currently working as an Assistant Professor with the Department of Electronics and Communication Engineering, KL University, Guntur, India. Her current research areas are MEMS and RF MEMS. She is currently working on MEMS project worth of 40 Lakhs, funded by SERB, Government of India. She has published over 25 International research publications, and presented over five conference technical papers around the world.

K. V. VINEETHA was born in Kerala, India. She received the bachelor's degree in electronics and instrumentation engineering from JNTUK, in 2016, and the master's degree in VLSI from KL University, in 2018, where she is currently pursuing the Ph.D. degree on MEMS research domain. She has published 11 International research publications, and has presented over three conference technical papers around the world.

P. ASHOK KUMAR was born in Andhra Pradesh, India. He received the bachelor's degree in electronics and communication engineering from JNTUH, in 2012, and the master's degree in VLSI from KL University, in 2017, where he is currently pursuing the Ph.D. degree on MEMS research domain. He has published 20 International research publications, and has presented more than five conference technical papers around the world.

D. PRATHYUSHA was born in Andhra Pradesh, India. She received the bachelor's degree in electronics and communication engineering from SCSVMV University, Kanchi, in 2016. She is currently pursuing the master's degree in VLSI with KL deemed to be University, Department of Electronics and Communication Engineering, KL University, Guntur, India. She is currently doing a project in the area of MEMS. She has attended a conference and published a paper, and one paper is under the review in Springer.

G. SAI LAKSHMI was born in Andhra Pradesh, India. She received the bachelor's degree in electronics and instrumentation engineering from JNTUK, in 2016. She is currently pursuing the master's degree in VLSI with KL deemed to be University, Department of Electronics and Communication Engineering, KL University, Guntur, India. She is currently doing a project in the area of MEMS. She has attended a conference and published a paper, and one paper is under the review in Springer.

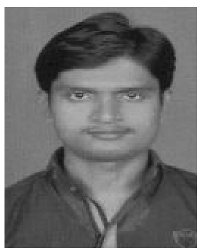

C. H. GOPI CHAND was born in Andhra Pradesh, India. He received the bachelor's degree in electronics and communication engineering from JNTUK, in 2016. He is currently pursuing the master's degree in VLSI with KL deemed to be University, Department of Electronics and Communication Engineering, KL University, Guntur, India. He is currently doing a project in the area of MEMS. He has attended a conference and published a paper, and one paper is under the review in Springer.

KOUSHIK GUHA received the B.Tech. degree in electronics and communication engineering from Techno India, Salt Lake, Kolkata, under the West Bengal University of Technology, India, in 2005, the M.Tech. degree in electronics and communication engineering (RF and Microwaves) from Burdwan University, West Bengal, India, in 2007, and the Ph.D. degree in design and modeling of RF MEMS shunt switch from NIT, Silchar, in 2016. He has worked as a Lecturer with the Department of ECE, Haldia Institute of Technology, West Bengal, India, from 2007 to 2010, and has served as a Visiting Faculty of NIT Mizoram, from 2012 to 2014. He is currently an Assistant Professor with the Electronics and Communication Engineering Department, National Institute of Technology, Silchar. He is a member of the IEEE and IETE.

• • •